Review article

Nuclear Medicine Communications

PET/CT in leukemia: utility and future directions

Akram Al-Ibraheem[a,b], Sudqi Allouzi[a], Ahmed Saad Abdlkadir[a], Miriam Mikhail-Lette[c], Kamal Al-Rabi[d], Mohammad Ma'koseh[d], Peter Knoll[e], Zaid Abdelrhman[d], Omar Shahin[d], Malik E. Juweid[f], Diana Paez[c] and Egesta Lopci[g]

2-Deoxy-2-[^{18}F]fluoro-D-glucose PET/computed tomography ([^{18}F]FDG PET/CT) has proven to be a sensitive method for the detection and evaluation of hematologic malignancies, especially lymphoma. The increasing incidence and mortality rates of leukemia have raised significant concerns. Through the utilization of whole-body imaging, [^{18}F]FDG PET/CT provides a thorough assessment of the entire bone marrow, complementing the limited insights provided by biopsy samples. In this regard, [^{18}F]FDG PET/CT has the ability to assess diverse types of leukemia The utilization of [^{18}F] FDG PET/CT has been found to be effective in evaluating leukemia spread beyond the bone marrow, tracking disease relapse, identifying Richter's transformation, and assessing the inflammatory activity associated with acute graft versus host disease. However, its role in various clinical scenarios in leukemia remains unacknowledged. Despite their less common use, some novel PET/CT radiotracers are being researched for potential use in specific scenarios in leukemia patients. Therefore, the objectives of this review are to provide a thorough assessment of the current applications of [^{18}F]FDG PET/CT in the staging and monitoring of leukemia patients, as well as the potential for an expanding role of PET/CT in leukemia patients. *Nucl Med Commun* 45: 550–563

Nuclear Medicine Communications 2024, **45**:550–563

Keywords: [^{18}F]FDG, chronic lymphocytic leukemia, extramedullary, leukemia, PET/CT, Richter's transformation

[a]Department of Nuclear Medicine and PET/CT, King Hussein Cancer Center (KHCC), [b]Department of Radiology and Nuclear Medicine, School of Medicine, University of Jordan, Amman, Jordan, [c]Nuclear Medicine and Diagnostic Imaging Section, Division of Human Health, Department of Nuclear Sciences and Applications, International Atomic Energy Agency, Vienna, Austria, [d]Department of Medical Oncology, King Hussein Cancer Center (KHCC), Amman, Jordan, [e]Dosimetry and Medical Radiation Physics Section, Division of Human Health, Department of Nuclear Sciences and Applications, International Atomic Energy Agency, Vienna, Austria, [f]Department of Radiology and Nuclear Medicine, University of Jordan, Amman, Jordan and [g]Department of Nuclear Medicine, IRCCS – Humanitas Clinical and Research Hospital, Rozzano (MI), Italy

Correspondence to Akram Al-Ibraheem, MD, FRCP, FEBNM, DCBNC, FANMB, Department of Nuclear Medicine, King Hussein Cancer Center (KHCC), P.O. Box 1269 Al-Jubeiha, Amman 11941, Jordan
Tel: +962 6 5300460x1104; e-mail: aibraheem@khcc.jo

Received 6 January 2024 **Accepted** 2 April 2024.

Introduction

Leukemia is a prevalent hematologic malignancy, comprising approximately 2.5% of newly diagnosed cancer cases and contributing to 3.1% of cancer-related mortality [1]. In leukemia, white blood cells proliferate uncontrollably, infiltrating the bone marrow with atypical cells that would render it dysfunctional [2]. As the disease progresses, infiltration of other sites and tissues is probable and would give rise to a wide spectrum of potential signs and symptoms that leukemia patients present with, also leading to significant morbidity and mortality, depending on the maturity and differentiation of the proliferating cells [3]. Leukemia can be classified into four major types as follows: acute lymphoblastic leukemia (ALL), acute myeloblastic leukemia (AML), chronic lymphocytic leukemia (CLL), and chronic myeloid leukemia (CML) [4]. Other subtypes include hairy cell leukemia (HCL), acute promyelocytic leukemia (APL), and the extremely aggressive therapy-refractory T-cell prolymphocytic leukemia (T-PLL) [5]. Diagnosing leukemia and assessing its potential spread to sites outside the bone marrow at early stages is essential for an adequate management and mitigation of the complications [6].

The utilization of 2-deoxy-2-[^{18}F]fluoro-D-glucose or 2-[^{18}F]fluoro-2-deoxy-D-glucose PET/computed tomography ([^{18}F]FDG PET/CT) in hematologic malignancies has been recently on the rise in the era of immunotherapy and novel agents [7]. In particular, the application of [^{18}F]FDG PET/CT has become very popular as a novel, noninvasive molecular imaging modality for the identification, staging, restaging, and evaluation of therapeutic response in hematologic malignancies, including lymphoma, myeloid sarcoma, and multiple myeloma [8–11]. In leukemia, [^{18}F]FDG PET/CT is of use in diagnosing, staging, restaging, assessing extramedullary involvement, follow up, and detecting Richter transformation [12]. However, its limitations mainly stems from the fact that [^{18}F]FDG uptake could be due to both malignant and benign conditions, along with the presence of areas that have high baseline metabolic activity, such as the brain, rendering [^{18}F]FDG of minimal usage in such areas [13].

Herein, we aim to review the current utility of PET/CT in the field of leukemia. Our focus will be on [^{18}F]FDG PET/CT, as it is the most commonly used radiotracer [5].

DOI: 10.1097/MNM.0000000000001846

A subsequent summary section will be dedicated to discussing other radiotracers utilized in this malignancy.

Leukemia: Patterns of FDG expression

[^{18}F]FDG-avid lesions on PET/CT are represented by their maximum standardized uptake value (SUVmax). As each leukemia subtype has variable metabolic activity, SUVmax values vary in acute and chronic leukemia. Indolent leukemias such as CLL exhibit SUVmax values between 1 and 4 [14–16]. However, if Richter transformation develops, SUVmax values become higher. In a retrospective series by Mauro *et al.*, the median SUVmax values were reported as 3.5 for CLL/small lymphocytic lymphoma (SLL), 14.6 for diffuse large B cell lymphoma (DLBCL), and 7.0 for Hodgkin lymphoma [17]. Falchi *et al.* reported a median SUVmax value of 3.7 for CLL, 6.8 for accelerated CLL, and 17.6 for Richter transformation [18]. Papajík *et al.* reported a median SUVmax value of 3.4 and 3.1 in new and relapsed CLL, respectively, vs. 16.5 in Richter transformation [19]. Regarding CML, two reported cases by Nakajo *et al.* showed diffuse bone marrow uptake [20]. Another CML case reported by Du *et al.* showed hepatic superscan in the liver with SUVmax of 24.3 and bone marrow SUVmax of 3.4 [21]. Arimoto *et al.* reported a bone marrow SUVmax of 4.3 in a CML patient [22].

In acute leukemia, some studies reported diffuse bone marrow uptake [21], while others reported multifocal uptake [23]. In a study by Zhou *et al.*, [^{18}F]FDG uptake was observed in 36 ALL lesions and 27 AML lesions, and the SUVmax was similar (7.0 ± 2.82 vs. 6.1 ± 2.29) for ALL and AML, respectively [24]. Kaya *et al.* reported the avidity of 38 extramedullary ALL lesions and found moderate avidity, with median SUVmax value of 5 (values ranged from 1.5 to 24.1) [25]. In a case series by Arimoto *et al.* that included six ALL patients, SUVmax ranged between 4.5 and 14 [22]. In two other ALL patients, one reported by Ciarallo *et al.* and the other by Arslan *et al.* SUVmax values were 7.5 and 8, respectively [26,27]. Su *et al.* reported a patient with four ALL lesions with SUVmax values ranging between 4.4 and 16 [28]. Several case series studies have reported AML lesions with SUVmax values ranging from 2.1 to 9.7 [29–31]. Kaya *et al.* reported 10 AML lesions with SUVmax values ranging between 1.5 and 7.5 [25].

For other subtypes of leukemia, Notarfranchi *et al.* reported a case of HCL with several sites of involvement that showed [^{18}F]FDG avidity with SUVmax of 4.9–10.9 [32]. Robak *et al.* performed [^{18}F]FDG PET/CT scan for HCL patient at the time of diagnosis and showed an SUVmax of 12.3 [33]. In the uncommon and aggressive T-PLL, Cheung *et al.* reported a case with hypermetabolic generalized lymphadenopathy and hepatosplenomegaly on [^{18}F]FDG PET/CT [34]. Based on previous studies, the obtained SUVmax values for different subtypes of leukemia exhibit diverse ranges with considerable overlaps, leading to difficulties in differentiating them (Table 1).

Utility of [^{18}F]FDG PET/CT in leukemia

The utility of [^{18}F]FDG PET/CT in leukemia diagnosis and management has been demonstrated in several studies. This section aims to provide a review of the existing literature on both acute and chronic leukemia.

Acute leukemia

These types progresses rapidly and aggressively and consist of AML, which is the predominant subtype among adult patients, and ALL, which is primarily prevalent among pediatrics [5].

Role in diagnosis

As the leukemic infiltration progresses through the bone marrow and other extramedullary tissues, signs and symptoms of leukemia start to become evident. In cases of acute leukemia patients might present with signs of bone marrow failure like anemia, infection, and bleeding [35]. However, in most instances patients would present with nonspecific symptoms that are usually attributed to more common etiologies [30].

Diagnosing leukemia can be difficult due to the various ways it can present and the locations of leukemic lesions, which may not be accessible through traditional physical examination methods [36]. A study involving 58 patients with ALL found that a lack of hematological symptoms can result in delays in diagnosis and suggested that PET/CT scans could be useful in such cases [37]. In some patients, leukemia can affect only a specific area of the bone marrow, leading to false-negative results in bone marrow biopsies. Arimoto *et al.* demonstrated that leukemia patients exhibit increased uptake of [^{18}F]FDG in their bone marrow, which could aid in diagnosis and help determine the most appropriate site for biopsy retrieval [22]. Alam *et al.* conducted a study which demonstrated that the infiltration of bone marrow by leukemia accounted for 35.5% of cases with elevated uptake, ranking second only to lymphoma at 45.2% [38]. Two separate case reports described patients who

Table 1 Degree of [^{18}F]FDG uptake in subtypes of leukemia

Leukemia subtype	Degree of [^{18}F]FDG uptake	Reported SUVmax range
CLL	None to mild	1–4
ALL	Mild to moderate	4–10
CML	Variable	3–25
AML	Mild to moderate	4–8

ALL, acute lymphoblastic leukemia; AML, acute myeloblastic leukemia; CLL, chronic lymphocytic leukemia; CML, chronic myeloid leukemia; FDG, fluorodeoxyglucose; SUVmax, maximum standardized uptake value.

initially presented with fever of unknown origin, but were later diagnosed with ALL through the use of [^{18}F]FDG PET/CT [27,28].

In AML, the role of [^{18}F]FDG PET/CT has been on the rise, especially after it has demonstrated its ability to detect extramedullary involvement. Myeloid sarcoma, which we will refer to as extramedullary acute myeloid leukemia (eAML), has been classically described in patients with AML. However, it was also seen in CML, myelodysplastic syndrome, and ALL and as an isolated tumor in the absence of intramedullary involvement [39]. Many sites of eAML involvement have been reported in the literature (Fig. 1) [40].

A clinical review has shown that eAML is often misdiagnosed as non-Hodgkin lymphoma (NHL) in up to 46% of cases [41]. Stölzel *et al.* demonstrated that [^{18}F]FDG had a sensitivity of 77% and a specificity of 97% with a positive predictive value of 83.3% in the detection of eAML [42]. A small case series has shown that [^{18}F]FDG PET/CT when paired with biopsies has a specificity of 80–90% with SUVmax values ranging from 2.1 to 9.7 [29,30,42].

Fig. 1

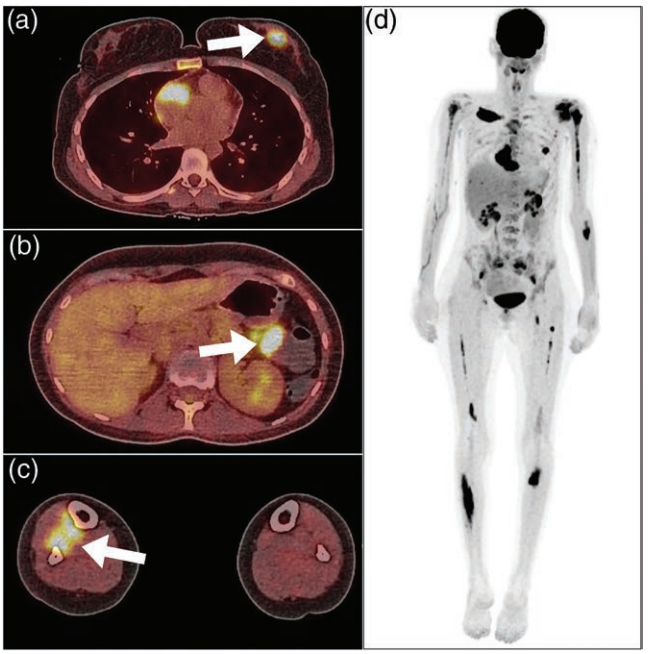

A 27-year-old female patient was diagnosed with acute myeloid leukemia (AML). [^{18}F]FDG PET/CT was performed for staging. (a–c) Fused axial PET/CT images of the chest, abdomen, and lower extremities demonstrate three extramedullary hypermetabolic lesions involving the left breast, descending colon, and left tibialis posterior muscle, respectively (arrows). (d) The MIP PET/CT image revealed multiple hypermetabolic medullary lesions coexisting with several extramedullary lesions. [^{18}F]FDG PET/CT, 2-deoxy-2-[^{18}F]fluoro-D-glucose PET/computed tomography; MIP, maximum intensity projection.

Role in staging and restaging

Staging of leukemia at diagnosis and restaging after treatment or progression or recurrence is essential to treating patients adequately. In a study by Zhou *et al.*, it was observed that the positive detection rate of [^{18}F]FDG PET/CT for extramedullary ALL was 88.9%, which helps in correctly staging ALL patients [24]. The same study also reported the sensitivity, specificity, and accuracy of [^{18}F]FDG PET/CT in diagnosing extramedullary involvement of ALL as 93.3%, 71.4%, and 79.7%, respectively [24]. In a case by Zhang *et al.*, a newly diagnosed 18-year-old patient with ALL underwent [^{18}F]FDG-PET/CT that revealed four extramedullary lesions previously undiscovered or suspected on clinical presentation or laboratory results [43]. In a study by Cunningham and Kohno, which included 16 patients with ALL, only 2 were found to have an isolated extramedullary lesion and 14 had multiple extramedullary lesions, emphasizing the importance of PET/CT's ability to scan the whole body to fully detect the true involvement of the malignancy [44].

In a study by Cribe *et al.* that included 26 AML patients, [^{18}F]FDG PET/CT revealed twice as many patients with extramedullary leukemia as found by clinical examination alone (65% vs. 31%) [29]. Fifty-five extramedullary lesions were found by PET/CT vs. 15 diagnosed by clinical examination, demonstrating that [^{18}F]FDG PET/CT is a useful tool for detecting and correctly staging leukemia [29]. The National Comprehensive Cancer Network recommends using [^{18}F]FDG PET/CT as the preferred imaging modality in suspected cases of eAML [45]. Bakst *et al.* concluded that [^{18}F]FDG PET/CT improves eAML detection, particularly in occult lesions [46]. In a 10-patient biopsy-proven eAML case series conducted by Stölzel *et al.*, PET/CT was able to detect eAML in 90% of patients and identify new extramedullary lesions in 60% of patients [42]. Moreover, 25 of the 27 extramedullary AMLs reported by Zhou *et al.* were avid on [^{18}F]FDG-PET/CT [24]. Cunningham and Kohno reviewed 101 PET/CT scans in patients with acute leukemia, and they concluded that the extent of leukemic involvement is significantly underestimated when a clinically apparent tumor is considered isolated and total body involvement is not sought by body scanning [44].

Role in follow-up, recurrence, and treatment response assessment

In a case by Cistaro *et al.*, a 9-year-old patient with ALL was evaluated for an isolated submandibular lymphadenopathy that was presumed to be an infection after no response to antibiotics. [^{18}F]FDG-PET/CT was performed, and the uptake pattern showed ALL recurrence in multiple lymph nodes, while the ultrasonography performed initially showed no suspicion for malignancy or recurrence of the primary disease [47]. Upon receiving treatment, follow-up PET/CT showed a reduction in

the [^{18}F]FDG uptake in the mentioned lesions [47]. In another case of ALL reported by Houghtelin *et al.*, an 18-year-old patient with ALL, who underwent peripheral blood hematopoietic cell transplantation, presented with breast pain and, upon performing [^{18}F]FDG PET/CT, abnormal uptake in bilateral breasts and multiple lymph nodes confirmed relapse [48]. Upon receiving appropriate chemotherapy follow up, [^{18}F]FDG PET/CT showed no evidence of increased uptake in the [^{18}F]FDG-avid areas in her initial scan [48]. Another case by Sonoki *et al.* reported a 35-year-old woman with ALL who presented with lower abdominal pain. [^{18}F]FDG-avid areas in both ovaries were present and were later found to represent ovarian relapse of ALL [49]. This case shows that PET scanning is a useful way to detect focal areas of leukemic relapse.

A case by Carli *et al.* demonstrated bilateral renal and myocardial involvement of ALL that was diagnosed and followed-up for complete resolution with the help of [^{18}F] FDG PET [50]. In a review by Cunningham and Kohno, which included 124 leukemic patients, PET/CT scans were conducted to evaluate treatment response following therapy [44]. A negative PET/CT scan was associated with favorable survival. However, ongoing monitoring was considered necessary as subsequent relapses occur in nearly 50% of the cases [44]. Kaya *et al.* suggested that combining [^{18}F]FDG PET/CT with bone marrow studies could enhance the detection of leukemic infiltration when recurrence or progression is suspected after treatment [25].

[^{18}F]FDG PET/CT has been gaining popularity in follow up and response assessment after patients receive treatment, as the definition of complete response includes the resolution of both bone marrow and, if present, extramedullary involvement (Fig. 2). Cunningham and Kohno [44], have reviewed 70 PET/CT scans after eAML patients had received various therapies (Table 2).

It is worth mentioning that there is limited evidence from large-scale studies supporting the role of tumor burden and PET parameter incorporation that is mandatory for response criteria adoption and accurate follow-up response assessment. In isolated eAML without intramedullary infiltration, 75–90% of patients would develop metachronous intramedullary AML within 4–12 months [40].

Chronic leukemia

These types progress slowly over time and consist of CLL, which is the predominant subtype, followed by the other subtype, which is CML.

Role in diagnosis

There has been some evidence in the literature that suggests the usefulness of [^{18}F]FDG-PET/CT in detecting CML; in two cases of CML reported by Nakajo *et al.*, patients had diffuse bone marrow uptake on [^{18}F]FDG PET/CT before treatment, and when followed up with a second PET/CT posttherapy initiation, reductions in [^{18}F]FDG uptake were noticed [20]. A case report by Varoglu *et al.* reported findings of [^{18}F]FDG-PET/CT scan performed in a renal cell carcinoma patient who revealed increased [^{18}F]FDG bone marrow uptake that helped in diagnosing CML [51]. Arimoto *et al.* also reported increased bone marrow [^{18}F]FDG uptake in a CML patient [22]. They observed a widespread and uniform distribution of [^{18}F]FDG uptake in the axial and upper peripheral skeleton, whereas the lower extremities exhibited localized areas of increased metabolic activity [22].

Currently, PET/CT scans are not regularly used for the diagnosis of suspected CLL due to its low metabolic activity (SUVmax of 1–4) and slow progression [52]. However, PET/CT scans can be effective in detecting accelerated CLL or more commonly Richter transformation due to their higher [^{18}F]FDG uptake [14–16,53].

Role in Richter's transformation

CLL is the most common leukemia among the elderly population, with a median age of onset of 70 years [54]. PET/CT is not routinely employed for the diagnosis of suspected CLL due to its low metabolic activity (SUVmax of 1–4) and indolent course [52]. As a result, PET/CT is of low avidity in cases of suspected CLL [14–16]. However, it is utilized in clinical practice to help detect a rare progression of CLL known as Richter transformation [55–58], a phenomenon first described by American hemopathologist Maurice Richter in 1928 [59]. Richter transformation is defined as the development of CLL into an aggressive lymphoma [60]. The incidence of Richter transformation ranges between 2% and 10% [61–64]. The two most common variants are DLBCL, accounting for 90% of cases, and Hodgkin lymphoma, accounting for approximately 10% of cases [65]. Transformation to histiocytic sarcoma, lymphoblastic leukemia, and interdigitating dendritic cell sarcoma has also been reported [66–69].

Richter transformation carries a poor prognosis, with median overall survival (OS) ranging from 2.5 to 10 months [70–76]. The median time to transformation in DLBCL is 1.8–1.9 years, while in Hodgkin lymphoma it is 4.6–7.5 years [77,78]. Given the catastrophic nature of this phenomenon, early diagnosis is crucial. In a retrospective series by Mauro *et al.*, the median SUVmax values were reported as 3.5 for CLL/SLL, 14.6 for DLBCL, 7.0 for Hodgkin lymphoma, and 6.3 for a secondary malignancy [17]. The CHOP-OR trial reported an SUVmax value of 18 in Richter transformation [79]. A median SUVmax value of 3.7 for CLL, 6.8 for accelerated CLL, and 17.6 for Richter transformation has been reported [18,19]. Whereas, a median SUVmax value of 3.4 and 3.1 in new and relapsed CLL with 16.5

Fig. 2

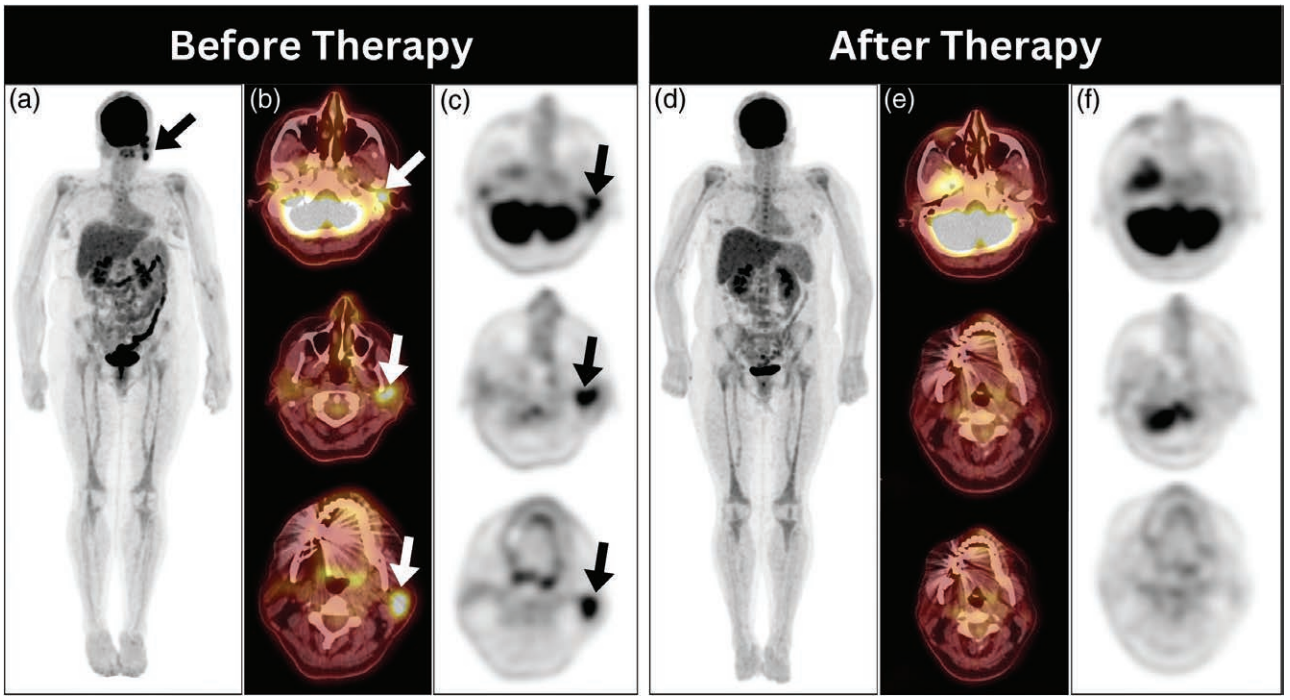

A 46-year-old female patient known to have myeloid sarcoma had [^{18}F]FDG PET/CT performed before and after intrathecal chemotherapy. (a–c) Pretherapeutic MIP, axial PET/CT, and axial PET images revealed evidence of a few hypermetabolic lesions occupying the left auditory canal and parotid gland (arrows). (d–f) Post-therapeutic MIP, axial PET/CT, and axial PET revealed evidence of a complete metabolic response. It is noteworthy that the diffuse bone marrow FDG uptake in this patient was due to a reactive process since multiple bone marrow biopsy samples were unremarkable. [^{18}F]FDG PET/CT, 2-deoxy-2-[^{18}F]fluoro-D-glucose PET/computed tomography; MIP, maximum intensity projection.

Table 2 Response assessment of multiple leukemic malignancies using [^{18}F]FDG PET/CT

Leukemia subtype	Number of cases	CR	PR	TR
AML	57	38	6	13
ALL	9	8	0	1

ALL, acute lymphoblastic leukemia; AML, acute myeloblastic leukemia; CR, complete response; PR, partial response; TR, treatment resistance.
Table was adapted from [44].

in Richter transformation has been reported [18,19]. A cut-off threshold of ≥5 SUVmax is the most commonly used value to suspect Richter transformation (Fig. 3) [80]. The initial investigation into the use of PET/CT for Richter transformation detection was conducted by Bruzzi *et al*. This study reported 91% sensitivity, 80% specificity, 54% positive predictive value, and 97% negative predictive value (NPV) while using the previously mentioned ≥5 SUVmax threshold [15]. In a recent systematic review conducted by Albano *et al*., which enrolled 13 studies using PET/CT to detect Richter transformation, an average overall sensitivity of 87%, specificity of 49%, positive predictive value of 41%, and NPV of 84% was reported [81]. The main source of false positives was non-transformed CLL [81]. Due to the high NPV provided by [^{18}F]FDG PET/CT, one can exclude Richter transformation if SUVmax is below 5. However, one cannot solely depend on [^{18}F]FDG PET/CT to detect its presence; in such cases, PET/CT can still help identify the index lesion, as the optimal biopsy site (Fig. 4) [82].

Falchi *et al*. demonstrated the potential prognostic value of PET/CT in Richter transformation, where the OS in patients with an SUVmax ≤10 was 56.7 months compared to an OS of 6.9 months for ≥10 [18]. It is important to note that some studies indicated that agents like BCL-2 inhibitors, BTKis, and anti-PD1 may influence the results (Table 3) [14].

Rare subtypes

For rare leukemic subtypes, the role of [^{18}F]FDG PET/CT is not quite documented or established with only a few reported cases to date. For PLL, Merdin *et al*. reported an acute case with visualized hypermetabolic supradiaphragmatic lymph nodes prior to therapy initiation [83]. Senthil *et al*. conducted a study on large granular lymphocytic (LGL) leukemia using [^{18}F]FDG PET/CT, which demonstrated the potential usefulness of this imaging technique in evaluating the disease extent and treatment response of aggressive forms of LGL leukemia [84]. Additionally, the effectiveness of [^{18}F]FDG PET/CT

Fig. 3

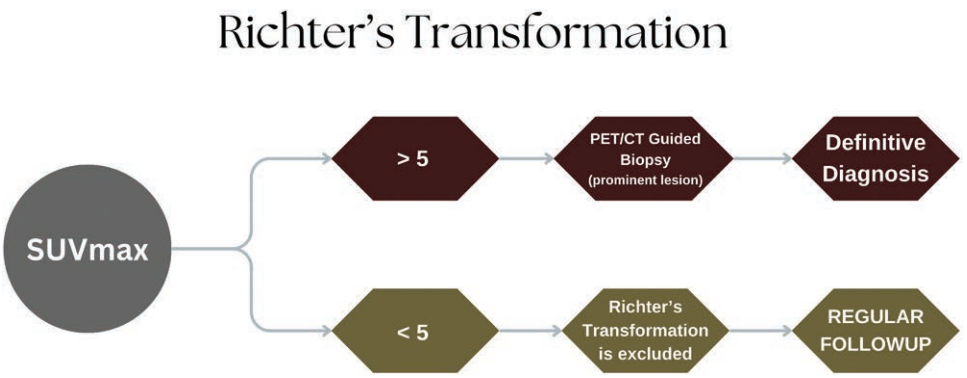

Simple diagram illustrating the proposed diagnostic scheme when assessing suspected cases for Richter's transformation.

Fig. 4

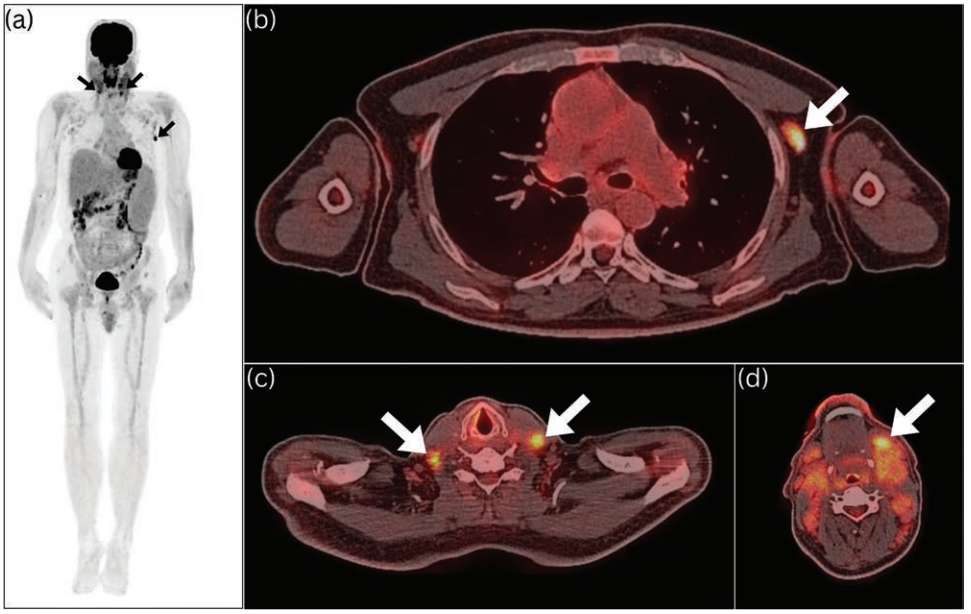

A 53-year-old male patient known to have had chronic lymphocytic leukemia (CLL) for the past 10 years. A recent suspicion of Richter's transformation necessitated further evaluation by [^{18}F] fluorodeoxyglucose PET/computed tomography ([^{18}F]FDG PET/CT). (a) Maximum intensity projection (MIP) image revealed evidence of a few hypermetabolic supradiaphragmatic lymph nodes having a maximum standardized uptake value exceeding 5 (SUVmax ranges from 5.9 to 11.1, arrows). (b–d) Axial PET/CT images of the chest, lower neck, and upper neck revealed evidence of a few hypermetabolic left axillary, left upper, and lower cervical lymph nodes, compatible with biopsy proven Richter's transformation.

was further confirmed in patients with extramedullary involvement in mast cell leukemia and chronic myelomonocytic leukemia [85,86]. In HCL, some studies suggest that [^{18}F]FDG PET/CT can serve as a useful imaging method for staging and evaluating treatment response [87–89]. Robak *et al.* reported that PET/CT is more sensitive and specific than a bone scan for assessing the response to chemotherapy [33]. In three studies on HCL, normalization of [^{18}F]FDG uptake was observed in all previously affected sites after treatment [32,90,91].

Other utilities

Role in detecting the extent of gastrointestinal graft versus host disease

Hematopoietic stem cell transplant (HSCT) is a significant therapeutic approach used to treat various types of blood cancers [92]. One of the most prevalent complications experienced by patients undergoing allo-HSCT is graft versus host disease (GVHD). GVHD occurs in approximately 30–50% of patients who undergo HSCT [93,94]. Gastrointestinal GVHD (GI-GVHD) is particularly common, affecting over 50–70% of individuals with

acute GVHD [95]. The identification of GI-GVHD can be challenging due to its nonspecific symptoms. Since GI-GVHD molecular imaging presentations can overlap with many other different etiologies, clinical and histopathological correlation have been used to attribute GI-GVHD hypermetabolic foci to GI-GVHD [96]. Bodet-Milin *et al.* found that [^{18}F]FDG PET/CT had a sensitivity of 81%, specificity of 90%, positive predictive value of 60%, and NPV of 96%, with an overall accuracy of 83% in detecting the extent of acute GI-GVHD (Fig. 5) [96]. A case reported by Dejanovic *et al.* demonstrated that [^{18}F]FDG PET/CT could be a valuable tool in detecting GVHD extent [97]; Stelljes *et al.* reported that PET/CT was able to detect GI-GVHD in 14 of 17 patients with biopsy-derived histological diagnoses [98]. Recently, Roll *et al.* retrospectively analyzed 101 patients with suspected GI-GVHD, and [^{18}F]FDG PET was able to detect its occurrence with a sensitivity of 93% and a specificity of 73% [99].

Role in assessing in-vivo drug pharmacokinetics

Cytokine-induced killer (CIK) is a type of immunotherapy used for various malignancies. Wang *et al.* enrolled nine patients with refractory APL, where pretreatment PET/CT revealed the tumor burden and increased uptake in a variety of sites [100]. They then radiolabeled CIK with [^{18}F]FDG and tracked its localization over regular intervals to assess its in-vivo kinetics, demonstrating that CIK is a tissue-targeted immunotherapy [100].

In another study, Kil *et al.* investigated the potential of [N-^{11}C-methyl]imatinib in evaluating the regional distribution and kinetics of imatinib within the human body [101]. The aim was to determine whether the drug effectively targets tumors and identify other organs where the drug or its labeled metabolites are distributed [101]. When used in conjunction with tracers like [^{18}F]FDG and [^{18}F]fluorothymidine ([^{18}F]FLT), [N-^{11}C-methyl]imatinib has the potential to serve as a valuable radiotracer for chemotherapy planning, monitoring treatment response, and assessing the impact of drug pharmacokinetics on drug resistance in CML [101].

Additionally, [^{18}F] can also be labeled with isocitrate dehydrogenase 1 (IDH1) [102]. Mutations in IDH1 have been observed in various malignancies, including AML [102]. Wang *et al.* [102] conducted a study where they successfully synthesized and evaluated two ^{18}F-labeled tracers, namely [^{18}F]AG120 and [^{18}F]AG135, for the purpose of visualizing the expression of mutated IDH1 in PET. Both tracers demonstrated favorable stability in laboratory settings, exhibited specific uptake in cells expressing mutated IDH1, and displayed promising pharmacokinetic characteristics with minimal uptake in most organs and tissues [102].

Role in disease prognostication

Some studies have focused on the prognostic value of the [^{18}F]FDG PET/CT findings in patients with leukemia; the prognostic significance of extramedullary involvement in leukemia is still being investigated [42]. A total of 12 patients with myeloid sarcoma who received radiotherapy were assessed by [^{18}F]FDG PET/CT before and after treatment [103]. In those patients, high pretreatment SUVmax was related to treatment failure. However, the sample size was small, and further studies in this field are, therefore warranted [103]. Zhao *et al.* analyzed a total of 79 scans from 72 patients with acute leukemia and found that the presence of extranodal, extramedullary, and extra-splenic sites was identified as an independent prognostic indicator [104]. Patients with this disease extent pattern were shown to have a lower OS rate in both univariate and multivariate survival analyses [104]. Therefore, incorporating [^{18}F]FDG PET/CT scans may be beneficial in identifying acute leukemia patients at higher risk for unfavorable clinical outcomes [104]. Porrazzo *et al.* conducted a study to assess the prognostic value of [^{18}F]FDG PET/CT in 40 CLL patients who had undergone chemotherapy [57]. Their findings indicated that patients with SUVmax greater than 5 had lower OS rates and were more prone to developing Richter's syndrome [57].

Additionally, studies have investigated the predictive value of [^{18}F]FDG PET/CT in aggressive CLL. Falchi *et al.* analyzed 764 CLL patients who underwent PET/CT scans for various reasons such as radiotherapy planning, initial staging, and treatment evaluation. They found that patients with lesions showing a SUVmax of ≥10 had a poorer OS. Similarly, Michallet *et al.* reported that CLL patients with hypermetabolic lesions with a SUVmax over 10 had higher mortality rates compared to those with a SUVmax below 10 [55]. Mato *et al.* conducted a retrospective analysis on pretreatment PET/CT scans of 167 CLL patients receiving venetoclax monotherapy [72]. They observed a longer progression-free survival in patients with a SUVmax below 10 compared to those with a SUVmax of 10 or higher [72]. In a more recent study, Albano *et al.* explored various parameters and cutoff thresholds to assess survival outcomes in patients with CLL [80]. After a median follow-up period of 32 months, 24 out of 80 patients died, with a mean time of 21.4 months (range, 1–130 months) [80]. Different cutoff thresholds for SUVmax adjusted for body weight and lean body mass (9 and 5.3, respectively), metabolic tumor volume (14.6), and total lesion glycolysis (40) were utilized in the survival analysis [80]. Patients with lesions exhibiting PET parameters above the specified cutoff thresholds were associated with poorer OS [80]. It is important to note that not all studies used the same cutoff thresholds; for instance, Mauro *et al.* observed inferior progression-free survival and OS in CLL patients with SUVmax ≥5 [17].

Table 3 Diagnostic accuracy of [^{18}F]FDG PET/CT in detecting Richter's transformation

Bruzzi *et al.*, 2006 [15]	
CLL cases	37
RT cases	11
SUVmax cutoff	5
Results	Sensitivity: 91%; specificity: 80%; PPV: 53%; NPV: 97%
Conclusion	Adopted cutoff is reliable for detecting Richter's transformation
Falchi *et al.*, 2014 [18]	
CLL cases	332
RT cases	95
SUVmax cutoff	5
Results	Sensitivity: 88%; specificity: 47%; PPV: 38%; NPV: 92%
Conclusion	PET/CT can be implemented to rule out Richter's transformation
Mauro *et al.*, 2015 [17]	
CLL cases	90
RT cases	17
SUVmax cutoff	5
Results	Sensitivity: 87%; specificity: 71%; PPV: 51%; NPV: 94%
Conclusion	The adopted cutoff has both prognostic and predictive significance
Michallet *et al.*, 2016 [55]	
CLL cases	240
RT cases	24
SUVmax cutoff	10
Results	Sensitivity: 91%; specificity: 95%; PPV: 29%; NPV: 99%
Conclusion	PET/CT can detect Richter's transformation and guide biopsies
Mato *et al.*, 2019 [58]	
CLL cases	57
RT cases	8
SUVmax cutoff	Multiple (5, 10, 11, 12)
Results	Sensitivity: 57–71%; specificity: 4–68%; PPV: 16–31%; NPV: 33–89%
Conclusion	The proposed cutoffs failed to predict Richter's transformation
Wang *et al.*, 2020 [56]	
CLL cases	92
RT cases	25
SUVmax cutoff	Multiple (5–10)
Results	Sensitivity: 56–96%; specificity: 21–76%; PPV: 51–69%; NPV: 67–86%
Conclusion	A biopsy should be performed in a patient with hypermetabolic lesions having SUVmax >5 to exclude Richter's transformation
Porrazzo *et al.*, 2020 [57]	
CLL cases	40
RT cases	5
SUVmax cutoff	5
Results	Sensitivity: 80%; Specificity: 74%; PPV: 31%; NPV: 96%
Conclusion	Adopted cutoff demonstrated vital prognostic and predictive values
Albano *et al.*, 2021 [80]	
CLL cases	80
RT cases	18
SUVmax cutoff	9
Results	Sensitivity: 67%; Specificity: 90%; PPV: 67%; NPV: 90%
Conclusion	SUV-related PET/CT predicted Richter's transformation

[^{18}F]FDG PET/CT, [^{18}F] fluorodeoxyglucose PET/computed tomography; CLL, chronic lymphocytic leukemia; NPV, negative predictive value; PPV, positive predictive value; RT, Richter's transformation; SUVmax, maximum standardized uptake value.

Role in patients with multiple primary neoplasms

[^{18}F]FDG PET/CT, due to its integration of both anatomical and functional imaging as well as the ability to scan the entire body, may offer certain benefits over traditional imaging techniques when evaluating patients with multiple primary malignant neoplasms. Paolini *et al.* have documented the valuable utility of [^{18}F]FDG PET/CT in individuals diagnosed with synchronous HCL and NHL [105]. The incidental identification of solid tumors alongside leukemic malignancies has also been previously documented [106].

Drawbacks and limitations

It is critical to understand that [^{18}F]FDG is a nonspecific tumor probe, and false positive findings are common in various presentations due to infectious and inflammatory conditions [107]. Furthermore, distinct nonspecific reactive patterns in bone marrow have been observed in a variety of clinical settings, including anemia and hematopoietic stimulating factors [38]. The accurate interpretation of these patterns in the clinical trajectory of the disease requires the expertise of the treating team. Despite the promising landscape in detecting Richter transformation and offering prognostic insights, it is crucial to acknowledge the limitations and drawbacks. The current manuscript text and accompanying simplified (Fig. 3) aim to present a straightforward perspective. Nevertheless, numerous authors have highlighted varying degrees of overlap and constraints when adopted certain SUVmax cutoff threshold [17,81].

Other radiotracers

Despite being less commonly used, some non-[^{18}F]FDG radiotracers are currently being investigated for their potential adoption in certain scenarios in leukemia patients. To date, there exist a limited literature render and acknowledgment in this domain.

[^{18}F]fluorothymidine

Buck *et al.* initially explored a thymidine analog with resistance to degradation in the human body in the context of leukemia [108]. Through a pilot study involving 10 patients, they observed a notably higher uptake of [^{18}F]FLT in the bone marrow of AML patients compared to controls (with average [^{18}F]FLT SUVmean of 11.5 vs. 6.6) [108]. Moreover, this analog had the potential to address the limitations of [^{18}F]FDG in detecting central nervous system involvement, which is hindered by the brain's high glucose hypermetabolism that can lead to falsely elevated SUV [109]. The analog's retention within the cells, facilitated by thymidine 1 kinase, can contribute to its specificity towards actively proliferating cellular populations [110].

Sanghera *et al.* discussed the use of [^{18}F]FLT PET before, during, and after treatment in patients with ALL [111]. The study found statistically significant differences between patients with complete remission and those with resistant disease, demonstrating the ability of [^{18}F]FLT to detect these differences within 2 days of initiating therapy [111]. Another study conducted by Agool *et al.* [112], reviewed 18 [^{18}F]FLT PET scans and concluded that [^{18}F]FLT offers both visual and quantitative information on the entire bone marrow, allowing for the differentiation of various bone marrow disorders and

Fig. 5

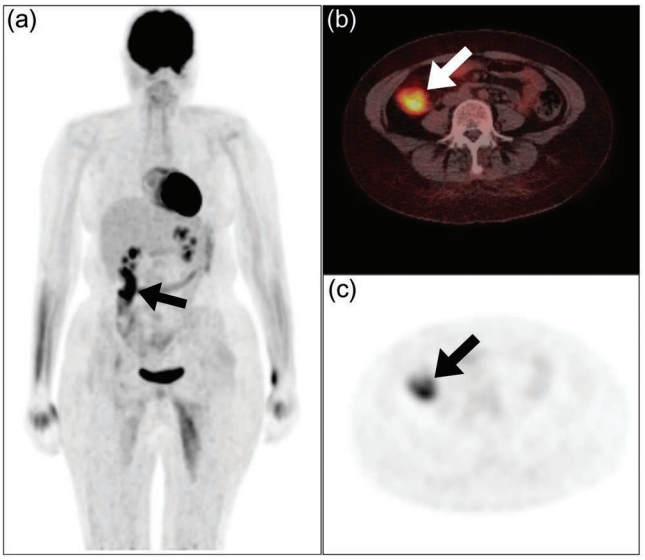

A 35-year-old female patient known to have acute lymphoblastic leukemia received many chemotherapy lines, followed by a recent allogenic stem cell transplant. A recent gastrointestinal complaint necessitated further evaluation by [^{18}F]FDG PET/CT to exclude graft versus host disease (GVHD). (a–c) MIP, axial PET/CT, and axial PET images revealed evidence of segmental hypermetabolic lesions occupying the ascending colon and hepatic flexure (arrows), compatible with biopsy proven gastrointestinal GVHD. [^{18}F]FDG PET/CT, [^{18}F] fluorodeoxyglucose PET/computed tomography.

potentially providing additional value in the posttreatment monitoring period [112]. At present, several clinical trials are underway employing [^{18}F]FLT PET/CT to assess different hematologic neoplasms (NCT00935090), diverse forms of leukemia (NCT01338987), and AML (NCT03422731).

[^{68}Ga]Ga-PentixaFor

The utilization of [^{68}Ga]Ga-PentixaFor has facilitated the nonintrusive PET visualization of CXCR4 expression [113]. Previous research has examined the recruitment and retention of leukemia-initiating cells, revealing that CXCR4 expression exerts a substantial influence on these processes [114]. Mayerhoefer *et al.* conducted an initial in-vivo application of a novel PET radiotracer that exhibits specificity towards CXCR4 expression [115]. Their study revealed an increased uptake of [^{68}Ga]Ga-PentixaFor in the bone marrow of patients diagnosed with CLL when compared to patients with other malignancies lacking bone marrow involvement [115]. The researchers deduced that [^{68}Ga]Ga-PentixaFor holds potential as a valuable tool for imaging CXCR4-dependent CLL.

Herhaus *et al.* [114] demonstrated that in-vivo imaging of myeloid malignancies, particularly AML, is achievable with [^{68}Ga]Ga-PentixaFor. In three patients, the correlation of CXCR4 imaging was assessed in comparison with its expression using immunohistochemistry, yielding promising findings [114]. However, due to the small sample size, a statistically significant correlation could not be established [114]. Buck *et al.* enrolled a larger cohort, comprising 690 participants with different cancer subtypes [116]. All patients underwent the [^{68}Ga]Ga-PentixaFor study for evaluation [116]. The findings of this study demonstrated that [^{68}Ga]Ga-PentixaFor exhibited the most pronounced uptake in hematologic malignancies, including ALL patients [116]. Habringer *et al.* demonstrated that the utilization of [^{68}Ga]Ga-PentixaFor facilitated the visualization of CXCR4 leukemic burden, thereby enabling the development of a theranostic approach for CXCR4 directed endoradiotherapy [117]. An ongoing clinical trial has been structured to investigate the potential of [^{68}Ga]Ga-PentixaFor in the treatment of lymphoma, leukemia, and multiple myeloma (NCT04504526).

Choline PET tracers

The process by which choline PET tracers are absorbed involves the targeting of choline transporters, which are increased in cancerous cells [118]. The choline transporter-like proteins CTLs/SLC44 family are abundantly present in different types of cancers, and their presence is linked to the survival of the cells [118]. Given the encouraging research on the efficacy of [^{11}C]Choline in prostate cancer and other malignant conditions, the limited absorption of [^{11}C]Choline in the brain could potentially aid in the detection of extramedullary leukemia in the central nervous system [119,120]. A case study conducted by Qin *et al.* illustrated the diagnosis of extramedullary brain AML using [^{11}C]Choline PET/CT, whereas [^{18}F]FDG PET/CT showed uptake levels comparable to those observed in surrounding healthy brain tissue [121]. Cegla *et al.* examined 1345 prostate cancer patients with multiple primary neoplasms using [^{18}F]Fluorocholine ([^{18}F]FCH) to assess the presence of coexisting CLL [122]. The researchers observed CLL lesions in two patients, both of whom displayed mild uptake with SUVmax of around 4 [122]. One year later, Kudura *et al.* documented the incidental identification of CLL in a left cervical lymph node showing mild [^{18}F]FCH uptake in a patient suspected to have a parathyroid adenoma [123]. The researchers advocated for additional research into the use of [^{18}F]FCH imaging in CLL patients to fully understand its diagnostic capabilities [123].

[^{68}Ga]Ga-DOTATATE

The utilization of [^{68}Ga]Ga-DOTA-conjugated peptides for somatostatin receptor (SSTR) imaging is well established in the field of diagnosing and evaluating the treatment response of neuroendocrine tumors [124]. This imaging technique also serves theranostic purposes [124]. SSTR expression has been observed in various benign and malignant pathologies, including lymphomas [125].

A recent case report denoted the incidental discovery of an intense [^{68}Ga]Ga-DOTATATE-avid vertebral lesion confirmed later by biopsy to be involved in CLL [126]. However, such an observation was singular, requiring further research to establish its significance.

[^{68}Ga]Ga-fibroblast activation protein inhibitor

The fibroblast activation protein inhibitor (FAPI) is classified as a type II integral membrane glycoprotein and has been recognized as a significant biomarker in cancer-associated fibroblasts [127]. Its level of expression is significantly increased in areas where tissue remodeling and tumor stroma occur [127]. FAPI has demonstrated potential in imaging different forms of cancer. Nonetheless, there is a scarcity of information regarding the use of [^{68}Ga]Ga-FAPI PET/CT, specifically for leukemia. The majority of existing studies concentrate on solid tumors, including lung cancer, colorectal cancer, and gynecological malignancies [128]. Consequently, the effectiveness of this innovative theranostic approach for leukemia remains uncertain. A recent case report conducted by Wu *et al.* validated the diagnostic usefulness of [^{68}Ga]Ga-FAPI PET/CT in a patient with myeloid sarcoma [129]. An intense [^{68}Ga]Ga-FAPI-avid left breast lesion was visualized before therapy, and posttreatment imaging using [^{68}Ga]Ga-FAPI PET/CT demonstrated disease regression affirming its applicability in similar cases [129]. In this specific case, the myeloid sarcoma lesions demonstrated a significantly higher degree of [^{68}Ga]Ga-FAPI uptake when compared to [^{18}F]FDG [129]. Moreover, [^{68}Ga]Ga-FAPI exhibited a superior tumor to background ratio in surrounding tissue, making it a valuable tool for visualizing myeloid sarcoma [129]. Cui *et al.* conducted a review in which they observed a patient diagnosed with eosinophilic leukemia who presented with eosinophilic myocarditis, a prevalent complication affecting approximately half of eosinophilic leukemia patients [130]. The patient underwent a [^{68}Ga]Ga-FAPI PET scan, revealing significant cardiac uptake initially, which subsequently resolved following treatment [130]. This finding highlights the potential value of [^{68}Ga]Ga-FAPI PET imaging in evaluating treatment response in such cases [130]. In general, additional research regarding [^{68}Ga]Ga-FAPI landscape in leukemia is imperative to substantiate these observations and explore the broader applications of this promising therapeutic and diagnostic agent.

Future Trends

In the field of leukemia, the near future looks promising given the recent shift in direction towards adopting artificial intelligence and immunoPET.

The value of artificial intelligence

Despite limited efforts focusing on this scope for the time being, it is expected that the field of artificial intelligence will dominate many aspects of molecular imaging implementation, especially in areas of uncertainty [131]. Notably, the value of machine learning and radiomics has been established in other forms of hematologic malignancies [132,133]. In an attempt to improve the diagnostic performance of [^{18}F]FDG PET/CT in detecting bone marrow lesions in leukemic patients, Li *et al.* conducted a retrospective study of 41 patients with acute leukemia [134]. All patients underwent both bone marrow biopsy and [^{18}F]FDG PET/CT within 1 week [134]. The bone marrow biopsy results were used as the gold standard for reference [134]. The skeletal volumes of interest were manually drawn on PET/CT images, and a total of 781 PET and 1045 CT radiomic features were automatically extracted to provide a more comprehensive understanding of the embedded pattern [134]. Through machine learning, they succeeded in achieving optimal sensitivity, specificity, and accuracy exceeding 85% for each [134]. This was significantly higher than relying solely on visual analysis ($P < 0.05$) [134]. Therefore, [^{18}F]FDG PET/CT radiomic analysis with a machine learning model can provide a quantitative, objective, and efficient mechanism for identifying bone marrow lesions in patients with suspected relapsed AL.

ImmunoPET

ImmunoPET is a molecular imaging technique that combines the high sensitivity and resolution of PET with the specificity of antibody-based targeting elements of the immune system and/or immune checkpoints [135]. While most of the research and applications of immunoPET have focused on solid tumors, there is also potential for its use in leukemia imaging. Some studies have explored its potential in this context. For example, a study evaluated immunoPET using [^{64}Cu]Cu-DOTA-Anti-CD33 PET-CT imaging in an AML xenograft model, demonstrating its potential for AML imaging [136]. [^{18}F] can also be linked to monoclonal antibodies (mAb) in order to assess their behavior within the body. In a recent investigation, researchers devised a partially automated technique to produce [^{18}F]-labeled anti-CD66, allowing for PET study to be conducted for the purpose of evaluating radiation dosage and examining the bone marrow [137]. The labeled antibody exhibited a tendency to accumulate primarily in the bone marrow, rendering it well suited for immunoPET investigations [137]. Glekas *et al.* sought to create an [^{18}F]-labeled analog of imatinib, not for imaging purposes, but as a tracer to track in-vivo drug distribution and concentration [138]. The synthesized 2-fluoroethyl analog, known as SKI696, demonstrated similar selectivity and binding affinity to imatinib in binding assays [138].

Alternatively, Madabushi *et al.* conducted a study using [^{64}Cu]Cu-DOTA-anti-CD33 murine mAb for immunoPET imaging of AML in a preclinical model [139]. The results showed high sensitivity and specificity,

highlighting spatial heterogeneity in the disease based on disease burden [139]. This suggests caution in interpreting results from single bone marrow biopsies [139]. The findings support the potential use of this imaging modality for noninvasive detection of AML in humans and monitoring treatment response [139]. Subsequent research by Allen *et al*. focused on [^{89}Zr]Zr-labeled lintuzumab molecule, showing promising results in PET imaging of CD33 positive human AML tumors [140]. These results align with ex-vivo biodistribution studies, indicating the potential of PET imaging with [^{89}Zr]Zr-lintuzumab as a tool for evaluating anti-CD33 mAb binding properties in preclinical cancer models [140].

Chimeric antigen receptor (CAR-T) cells are a crucial component of leukemia immunotherapy [7]. Wang *et al*. conducted a study demonstrating the feasibility of labeling CAR-T cells with [^{68}Ga]Ga-oxine for in-vivo tracking through PET imaging [141]. Additionally, CAR-T cells labeled with [^{89}Zr]Zr-oxine were utilized for long-term monitoring [141]. This methodology was employed in mice to track CAR-T cell distribution via PET imaging and confirmed through ex-vivo analysis [141]. Programmed cell death-ligand 1 (PD-L1) is commonly found in various types of cancer, including leukemia [142]. Sun *et al*. developed a new peptide imaging agent called Al[^{18}F]-NOTA-IPB-PDL1P, which targets PD-L1 in tumors specifically [142]. Their findings suggest that this agent has the potential to be used for PET imaging of tumors with high levels of PD-L1 expression [142]. In contrast, Jung *et al*. created an immune PET imaging agent labeled with [^{89}Zr]Zr that targets PD-L1 and can monitor changes in PD-L1 expression in tumors following chemotherapy treatment [143]. The synthesis of [^{89}Zr]Zr-anti-PD-L1 was efficient and the imaging properties were favorable [143]. Treatment with gemcitabine resulted in an increase in PD-L1 expression in cancer cells and tumors, leading to enhanced uptake of [^{89}Zr]Zr-anti-PD-L1 [143]. This PET imaging agent has the potential to be a valuable tool for tracking changes in tumor PD-L1 expression in response to chemotherapy in living subjects [143]. In order to measure PD-L1 levels without invasive methods, Mishra *et al*. developed a new peptide-based binder called [^{68}Ga]Ga-DK223 [144]. They investigated the distribution, pharmacokinetics, and specificity of [^{68}Ga]Ga-DK223 *in vivo* in diverse neoplasms, which exhibit varying levels of PD-L1 expression [144]. [^{68}Ga]Ga-DK223 produced clear PET images within an hour of administration and demonstrated the ability to detect PD-L1 in xenograft models in a manner that is dependent on its expression levels [144]. The researchers concluded that [^{68}Ga]Ga-DK223-PET could be a valuable tool for accurately measuring both baseline PD-L1 levels and accessible PD-L1 levels during therapy, allowing for a better understanding of drug exposure at the tumor site [144]. This supports the potential use of [^{68}Ga]Ga-DK223-PET for guiding and optimizing immune checkpoint therapy [144].

Conclusion

In conclusion, PET/CT is a noninvasive and accessible imaging technique that holds great potential in the field of leukemia. Its utilization has resulted in the early identification of Richter transformation, a particularly unfavorable outcome in patients with CLL. Furthermore, PET/CT has been successful in uncovering hidden extramedullary leukemic involvement that may have been overlooked during clinical examinations or conventional CT/MRI scans. This capability has the potential to enhance the development of personalized treatment plans for patients, particularly those with atypical presentations. The advantages of PET/CT in detecting disease recurrence, assessing treatment response, and monitoring for GVHD could greatly advance its utilization in clinical practice.

The development of novel radiotracers could address some of the limitations of [^{18}F]FDG PET/CT by improving the ability to differentiate between benign and malignant conditions and enhancing extramedullary detection within the brain. Furthermore, the adoption of artificial intelligence and immunoPET can enhance the reliability of this imaging technique. However, prospective and large studies of PET/CT applications in leukemia are still lacking, which could be hindering the exploration of their full potential in leukemic patients.

Acknowledgements

A.A.-I., S.A., A.S.A., M.E.J., D.P., and E.L. have made substantial contributions to concept and design of the study. A.A.-I., S.A., and A.S.A. carried out analysis of data and wrote the manuscript. A.A.-I., A.S.A., K.A.-R., and M.M. prepared the figures. A.A.-I., M.M.-L., P.K., Z.A., and O.S. were in charge of editing the manuscript. The final paper was read and approved by all authors.

Conflicts of interest

There are no conflicts of interest.

References

1 Sung H, Ferlay J, Siegel RL, Laversanne M, Soerjomataram I, Jemal A, *et al*. Global cancer statistics 2020: GLOBOCAN estimates of incidence and mortality worldwide for 36 cancers in 185 countries. *CA Cancer J Clin* 2021; **71**:209–249.
2 Riether C, Schürch C, Ochsenbein A. Regulation of hematopoietic and leukemic stem cells by the immune system. *Cell Death Differ* 2015; **22**:187–198.
3 Rappaport H. *Tumors of the hematopoietic system*. Armed Forces Institute of Pathology; 1966.
4 Zerbini MCN, Soares FA, Velloso EDRP, Paes RP. World Health Organization classification of tumors of hematopoietic and lymphoid tissues, 2008 – major changes from the 3rd edition, 2001. *Rev Assoc Med Bras* 2011; **57**:66–73.
5 Mayerhoefer ME, Archibald SJ, Messiou C, Staudenherz A, Berzaczy D, Schöder H. MRI and PET/MRI in hematologic malignancies. *J Magn Reson Imaging* 2020; **51**:1325–1335.

6 Whiteley AE, Price TT, Cantelli G, Sipkins DA. Leukaemia: a model metastatic disease. *Nat Rev Cancer* 2021; **21**:461–475.
7 Al-Ibraheem A, Abdlkadir AS, Juweid ME, Al-Rabi K, Ma'koseh M, Abdel-Razeq H, *et al*. FDG-PET/CT in the monitoring of lymphoma immunotherapy response: current status and future prospects. *Cancers (Basel)* 2023; **15**:1063.
8 Al-Ibraheem A, Anwer F, Juweid ME, Shagera QA, Khalaf AN, Obeidat S, *et al*. Interim FDG-PET/CT for therapy monitoring and prognostication in Hodgkin's lymphoma. *Sci Rep* 2022; **12**:17702.
9 Taghipour M, Marcus C, Nunna P, Subramaniam RM. Follow-up FDG PET/CT in patients with non-Hodgkin lymphoma: value to clinical assessment and patient management. *Clin Nucl Med* 2016; **41**:e93–e97.
10 Lee EYP, Anthony M-P, Leung AY-H, Loong F, Khong P-L. Utility of FDG PET/CT in the assessment of myeloid sarcoma. *AJR Am J Roentgenol* 2012; **198**:1175–1179.
11 Agarwal A, Chirindel A, Shah BA, Subramaniam RM. Evolving role of FDG PET/CT in multiple myeloma imaging and management. *AJR Am J Roentgenol* 2013; **200**:884–890.
12 Zhao Z, Hu Y, Li J, Zhou Y, Zhang B, Deng S. Applications of PET in diagnosis and prognosis of leukemia. *Technol Cancer Res Treat* 2020; **19**:1533033820956993.
13 Sarji SA. Physiological uptake in FDG PET simulating disease. *Biomed Imaging Interv J* 2006; **2**:e59–e60.
14 Musanhu E, Sharma R, Attygalle A, Wotherspoon A, Chau I, Cunningham D, *et al*. Chronic lymphocytic leukaemia and Richter's transformation: multimodal review and new imaging paradigms. *Clin Radiol* 2021; **76**:789–800.
15 Bruzzi JF, Macapinlac H, Tsimberidou AM, Truong MT, Keating MJ, Marom EM, *et al*. Detection of Richter's transformation of chronic lymphocytic leukemia by PET/CT. *J Nucl Med* 2006; **47**:1267–1273.
16 Karam M, Novak L, Cyriac J, Ali A, Nazeer T, Nugent F. Role of fluorine-18 fluoro-deoxyglucose positron emission tomography scan in the evaluation and follow-up of patients with low-grade lymphomas. *Cancer* 2006; **107**:175–183.
17 Mauro F, Chauvie S, Paoloni F, Biggi A, Cimino G, Rago A, *et al*. Diagnostic and prognostic role of PET/CT in patients with chronic lymphocytic leukemia and progressive disease. *Leukemia* 2015; **29**:1360–1365.
18 Falchi L, Keating MJ, Marom EM, Truong MT, Schlette EJ, Sargent RL, *et al*. Correlation between FDG/PET, histology, characteristics, and survival in 332 patients with chronic lymphoid leukemia. *Blood* 2014; **123**:2783–2790.
19 Papajík T, Mysliveček M, Urbanová R, Buriánková E, Kapitáňová Z, Procházka V, *et al*. 2-[18F] fluoro-2-deoxy-D-glucose positron emission tomography/computed tomography examination in patients with chronic lymphocytic leukemia may reveal Richter transformation. *Leuk Lymphoma* 2014; **55**:314–319.
20 Nakajo M, Jinnouchi S, Inoue H, Otsuka M, Matsumoto T, Kukita T, *et al*. FDG PET findings of chronic myeloid leukemia in the chronic phase before and after treatment. *Clin Nucl Med* 2007; **32**:775–778.
21 Du B, Li X, Li N, Li Y, Hsu B. 18F-FDG hepatic superscan in a patient with chronic myeloid leukemia. *Clin Nucl Med* 2014; **39**:835–836.
22 Arimoto MK, Nakamoto Y, Nakatani K, Ishimori T, Yamashita K, Takaori-Kondo A, *et al*. Increased bone marrow uptake of 18F-FDG in leukemia patients: preliminary findings. *Springerplus* 2015; **4**:1–6.
23 Bartakke S, Abdelhaleem M, Abla O. Childhood acute lymphoblastic leukaemia simulating multifocal osteomyelitis. *Br J Haematol* 2007; **139**:2.
24 Zhou W-l, Wu H-b, Wang L-j, Tian Y, Dong Y, Wang Q-s. Usefulness and pitfalls of F-18-FDG PET/CT for diagnosing extramedullary acute leukemia. *Eur J Radiol* 2016; **85**:205–210.
25 Kaya Z, Akdemir OU, Atay OL, Akyürek N, Pınarlı FG, Yenicesu I, *et al*. Utility of 18-fluorodeoxyglucose positron emission tomography in children with relapsed/refractory leukemia. *Pediatr Hematol Oncol* 2018; **35**:393–406.
26 Ciarallo A, Makis W, Novales-Diaz J-A, Michel RP. Extramedullary gastric relapse of acute lymphoblastic leukemia following allogeneic stem cell transplant: staging with F-18 FDG PET/CT. *Clin Nucl Med* 2011; **36**:e90–e92.
27 Arslan F, Yilmaz M, Çakir T, Mert A. Significant contribution of fluorodeoxyglucose positron emission tomography/computed tomography (FDG PET/CT) in a case of acute lymphoblastic leukemia presenting with fever of unknown origin. *Intern Med* 2014; **53**:789–791.
28 Su K, Nakamoto Y, Nakatani K, Kurihara K, Hayakawa N, Togashi K. Diffuse homogeneous bone marrow uptake of FDG in patients with acute lymphoblastic leukemia. *Clin Nucl Med* 2013; **38**:e33–e34.
29 Cribe ASWI, Steenhof M, Marcher CW, Petersen H, Frederiksen H, Friis LS. Extramedullary disease in patients with acute myeloid leukemia assessed by (18) F-FDG PET. *Eur J Haematol* 2013; **90**:273–278.
30 Ueda K, Ichikawa M, Takahashi M, Momose T, Ohtomo K, Kurokawa M. FDG-PET is effective in the detection of granulocytic sarcoma in patients with myeloid malignancy. *Leuk Res* 2010; **34**:1239–1241.
31 Stölzel F, Röllig C, Radke J, Mohr B, Platzbecker U, Bornhäuser M, *et al*. 18F-FDG-PET/CT for detection of extramedullary acute myeloid leukemia. *Haematologica* 2011; **96**:1552–1556.
32 Notarfranchi L, Russo F, Re F, Mancini C, Martella E, Falini B, *et al*. Hairy cell leukaemia mimicking multiple myeloma. *Lancet Oncol* 2019; **20**:e187.
33 Robak P, Jesionek-Kupnicka D, Kupnicki P, Polliack A, Robak T. Bone lesions in hairy cell leukemia: diagnosis and treatment. *Eur J Haematol* 2020; **105**:682–691.
34 Cheung CY, Leung RY, Tam AR, Sim JP, Kwong Y-l. Disseminated Mycobacterium haemophilum infection during alemtuzumab treatment of T-cell prolymphocytic leukemia. *Ann Hematol* 2023; **102**:483–485.
35 Chennamadhavuni A, Lyengar V, Mukkamalla SKR, Shimanovsky A. *Leukemia*. StatPearls; 2023.
36 Chiaretti S, Zini G, Bassan R. Diagnosis and subclassification of acute lymphoblastic leukemia. *Mediterr J Hematol Infect Dis* 2014; **6**:e2014073.
37 Ikawa Y, Takenaka M, Sakai Y, Noguchi K, Fukuda M, Fujiki T, *et al*. Utility of 18F-FDG-PET for detecting acute lymphoblastic leukemia: a case series of pediatric acute lymphoblastic leukemia without hematological symptoms. *Int J Hematol* 2022; **115**:287–292.
38 Alam MS, Fu L, Ren Y-Y, Wu H-B, Wang Q-S, Han Y-J, *et al*. 18F-FDG super bone marrow uptake: a highly potent indicator for the malignant infiltration. *Medicine (Baltimore)* 2016; **95**:e5579.
39 Eshghabadi M, Shojania AM, Carr I. Isolated granulocytic sarcoma: report of a case and review of the literature. *J Clin Oncol* 1986; **4**:912–917.
40 Shallis RM, Gale RP, Lazarus HM, Roberts KB, Xu ML, Seropian SE, *et al*. Myeloid sarcoma, chloroma, or extramedullary acute myeloid leukemia tumor: a tale of misnomers, controversy and the unresolved. *Blood Rev* 2021; **47**:100773.
41 Byrd JC, Edenfield WJ, Shields DJ, Dawson NA. Extramedullary myeloid cell tumors in acute nonlymphocytic leukemia: a clinical review. *J Clin Oncol* 1995; **13**:1800–1816.
42 Stölzel F, Lüer T, Löck S, Parmentier S, Kuithan F, Kramer M, *et al*. The prevalence of extramedullary acute myeloid leukemia detected by 18FDG-PET/CT: final results from the Prospective PETAML Trial. *Haematologica* 2020; **105**:1552–1558.
43 Zhang S, Wang W, Kan Y, Liu J, Yang J. Extramedullary infiltration of acute lymphoblastic leukemia in multiple organs on FDG PET/CT. *Clin Nucl Med* 2018; **43**:217–219.
44 Cunningham I, Kohno B. 18FDG-PET/CT: 21st century approach to leukemic tumors in 124 cases. *Am J Hematol* 2016; **91**:379–384.
45 Goyal H, Jain S. Applications of 18F-FDG PET/CT in lymphoma and leukemia with focus on NCCN guidelines: a pictorial review. *J Nuclear Med* 2023; **64**:P1123–P1124.
46 Bakst R, Powers A, Yahalom J. Diagnostic and therapeutic considerations for extramedullary leukemia. *Curr Oncol Rep* 2020; **22**:1–7.
47 Cistaro A, Saglio F, Asaftei S, Fania P, Berger M, Fagioli F. The role of 18F-FDG PET/CT in pediatric lymph-node acute lymphoblastic leukemia involvement. *Radiol Case Rep* 2011; **6**:503.
48 Houghtelin AB, Kopp LM, Pelayo-Katsanis L, Kuo PH, Yeager AM, Katsanis E. Extramedullary breast relapse of acute lymphoblastic leukemia controlled with a second allogeneic/autologous hematopoietic cell transplant. *J Adolesc Young Adult Oncol* 2015; **4**:50–53.
49 Sonoki T, Iwanaga E, Mitsuya H, Asou N. Ovarian relapse seven years after bone marrow transplantation for B-cell acute lymphoblastic leukemia: an unusual Krukenberg tumor. *Am J Hematol* 2005; **80**:75–76.
50 Carli G, Guardalben E, Bonifacio M, Meneghini V, Tecchio C, Cucca M, *et al*. PBX/E2A transcript positive B-lymphoblastic leukaemia (B-All) presenting with bilateral renal and myocardial involvement: a case report. *Haematologica* 2013; **98**:63.
51 Varoglu E, Kaya B, Sari O. Chronic myeloid leukemia detected on FDG PET/CT imaging in a patient with renal cell carcinoma. *Rev Esp Med Nucl Imagen Mol* 2013; **32**:43–45.
52 Conte M, Bowen D, Wiseman G, Rabe KG, Slager SL, Schwager SM, *et al*. Use of positron emission tomography-computed tomography in the management of patients with chronic lymphocytic leukemia/small lymphocytic lymphoma. *Leuk Lymphoma* 2014; **55**:2079–2084.
53 Juweid ME, Mueller M, Alhouri A, A-Risheq MZ, Mottaghy FM. Positron emission tomography/computed tomography in the management of Hodgkin and B-cell non-Hodgkin lymphoma: An update. *Cancer* 2021; **127**:3727–3741.

54 Noone A, Krapcho M, Miller D. *SEER Cancer Statistics Review (CSR) 1975-2015* (updated September 10, 2018); 2018.
55 Michallet A-S, Sesques P, Rabe KG, Itti E, Tordot J, Tychyj-Pinel C, *et al*. An 18F-FDG-PET maximum standardized uptake value >10 represents a novel valid marker for discerning Richter's syndrome. *Leuk Lymphoma* 2016; **57**:1474–1477.
56 Wang Y, Rabe KG, Bold MS, Shi M, Hanson CA, Schwager SM, *et al*. The role of 18F-FDG-PET in detecting Richter transformation of chronic lymphocytic leukemia in patients receiving therapy with a B-cell receptor inhibitor. *Haematologica* 2020; **105**:2675–2678.
57 Porrazzo M, Nicolai E, Riminucci M, Vitale C, Coscia M, De Paoli L, *et al*. Prognostic significance of PET/CT in patients with chronic lymphocytic leukemia (CLL) treated with frontline chemoimmunotherapy. *Cancers (Basel)* 2020; **12**:1773.
58 Mato A, Wierda W, Davids M, Cheson B, Coutre S, Choi M, *et al*. Utility of PET-CT in patients with chronic lymphocytic leukemia following B-cell receptor pathway inhibitor therapy. *Haematologica* 2019; **104**:2258–2264.
59 Richter MN. Generalized reticular cell sarcoma of lymph nodes associated with lymphatic leukemia. *Am J Pathol* 1928; **4**:285–292.7.
60 Swerdlow SH, Campo E, Harris NL, Jaffe ES, Pileri SA, Stein H, *et al*. *WHO classification of tumours of haematopoietic and lymphoid tissues*. International Agency for Research on Cancer; 2008.
61 Al-Sawaf O, Robrecht S, Bahlo J, Fink A, Cramer P, v Tresckow J, *et al*. Richter transformation in chronic lymphocytic leukemia (CLL)–a pooled analysis of German CLL Study Group (GCLLSG) front line treatment trials. *Leukemia* 2021; **35**:169–176.
62 Parikh SA, Kay NE, Shanafelt TD. How we treat Richter syndrome. *Blood* 2014; **123**:1647–1657.
63 Tsimberidou A-M, O'Brien S, Khouri I, Giles FJ, Kantarjian HM, Champlin R, *et al*. Clinical outcomes and prognostic factors in patients with Richter's syndrome treated with chemotherapy or chemoimmunotherapy with or without stem-cell transplantation. *J Clin Oncol* 2006; **24**:2343–2351.
64 Rossi D, Spina V, Deambrogi C, Rasi S, Laurenti L, Stamatopoulos K, *et al*. The genetics of Richter syndrome reveals disease heterogeneity and predicts survival after transformation. *Blood* 2011; **117**:3391–3401.
65 Khan M, Siddiqi R, Thompson PA. Approach to Richter transformation of chronic lymphocytic leukemia in the era of novel therapies. *Ann Hematol* 2018; **97**:1–15.
66 Trump DL, Mann RB, Phelps R, Roberts H, Conley CL. Richter's syndrome: diffuse histiocytic lymphoma in patients with chronic lymphocytic leukemia: a report of five cases and review of the literature. *Am J Med* 1980; **68**:539–548.
67 Shao H, Xi L, Raffeld M, Feldman AL, Ketterling RP, Knudson R, *et al*. Clonally related histiocytic/dendritic cell sarcoma and chronic lymphocytic leukemia/small lymphocytic lymphoma: a study of seven cases. *Mod Pathol* 2011; **24**:1421–1432.
68 Chakhachiro Z, Yin CC, Abruzzo LV, Aladily TN, Barron LL, Banks HE, *et al*. B-lymphoblastic leukemia in patients with chronic lymphocytic leukemia: a report of four cases. *Am J Clin Pathol* 2015; **144**:333–340.
69 Fraser CR, Wang W, Gomez M, Zhang T, Mathew S, Furman RR, *et al*. Transformation of chronic lymphocytic leukemia/small lymphocytic lymphoma to interdigitating dendritic cell sarcoma: evidence for transdifferentiation of the lymphoma clone. *Am J Clin Pathol* 2009; **132**:928–939.
70 Rossi D, Spina V, Cerri M, Rasi S, Deambrogi C, De Paoli L, *et al*. Stereotyped B-cell receptor is an independent risk factor of chronic lymphocytic leukemia transformation to Richter syndrome. *Clin Cancer Res* 2009; **15**:4415–4422.
71 Parikh SA, Rabe KG, Call TG, Zent CS, Habermann TM, Ding W, *et al*. Diffuse large B-cell lymphoma (Richter syndrome) in patients with chronic lymphocytic leukaemia (CLL): a cohort study of newly diagnosed patients. *Br J Haematol* 2013; **162**:774–782.
72 Mato AR, Nabhan C, Barr PM, Ujjani CS, Hill BT, Lamanna N, *et al*. Outcomes of CLL patients treated with sequential kinase inhibitor therapy: a real world experience. *Blood* 2016; **128**:2199–2205.
73 Ayers EC, Mato AR. Richter's transformation in the era of kinase inhibitor therapy: a review. *Clin Lymphoma Myeloma Leuk* 2017; **17**:1–6.
74 Jain P, Keating M, Wierda W, Estrov Z, Ferrajoli A, Jain N, *et al*. Outcomes of patients with chronic lymphocytic leukemia after discontinuing ibrutinib. *Blood* 2015; **125**:2062–2067.
75 Maddocks KJ, Ruppert AS, Lozanski G, Heerema NA, Zhao W, Abruzzo L, *et al*. Etiology of ibrutinib therapy discontinuation and outcomes in patients with chronic lymphocytic leukemia. *JAMA Oncol* 2015; **1**:80–87.
76 Tsimberidou AM, Wierda WG, Wen S, Plunkett W, O'Brien S, Kipps TJ, *et al*. Phase I–II clinical trial of oxaliplatin, fludarabine, cytarabine, and rituximab therapy in aggressive relapsed/refractory chronic lymphocytic leukemia or Richter syndrome. *Clin Lymphoma Myeloma Leuk* 2013; **13**:568–574.
77 Ahn IE, Underbayev C, Albitar A, Herman SE, Tian X, Maric I, *et al*. Clonal evolution leading to ibrutinib resistance in chronic lymphocytic leukemia. *Blood* 2017; **129**:1469–1479.
78 Parikh SA, Habermann TM, Chaffee KG, Call TG, Ding W, Leis JF, *et al*. Hodgkin transformation of chronic lymphocytic leukemia: incidence, outcomes, and comparison to de novo Hodgkin lymphoma. *Am J Hematol* 2015; **90**:334–338.
79 Eyre TA, Schuh A. An update for Richter syndrome–new directions and developments. *Br J Haematol* 2017; **178**:508–520.
80 Albano D, Camoni L, Rodella C, Giubbini R, Bertagna F. 2-[18F]-FDG PET/CT role in detecting Richter transformation of chronic lymphocytic leukemia and predicting overall survival. *Clin Lymphoma Myeloma Leuk* 2021; **21**:e277–e283.
81 Albano D, Bertagna F, Dondi F, Annunziata S, Ceriani L, Giovanella L, *et al*. The role of 2-[^{18}F]-FDG PET/CT in detecting Richter transformation in chronic lymphocytic leukemia: a systematic review. *Radiation* 2021; **1**:65–76.
82 Condoluci A, Rossi D. Biology and treatment of Richter transformation. *Front Oncol* 2022; **12**:829983.
83 Merdin A, Yıldız J, Dal Mehmet S, Çakar MK, Batgi H, Tekgündüz E, *et al*. A 80-year-old woman with B-cell prolymphocytic leukemia. *Hematol Rep* 2017; **9**:6995.
84 Senthil R, Pratap T, Mahadevan P, Gangadharan V. Atypical presentation of T-cell large granular lymphocytic leukemia mimicking pleural malignancy on 18F-FDG PET/CT. *Clin Nucl Med* 2019; **44**:e296–e2e7.
85 Fu Z, Zhang J, Liu M, Li Z, Li Q. Extramedullary involvement of mast cell leukemia detected by 18F-FDG PET/CT. *Clin Nucl Med* 2016; **41**:578–579.
86 Derlin T, Clauditz TS, Bannas P. 18F-FDG PET/CT for staging and detection of extramedullary organ involvement in chronic myelomonocytic leukemia. *Clin Nucl Med* 2014; **39**:811–812.
87 Rosen DS, Smith S, Gurbuxani S, Yamini B. Extranodal hairy cell leukemia presenting in the lumbar spine: case report. *J Neurosurg Spine* 2008; **9**:374–376.
88 Subhawong A, Subhawong T, Ali S. Hairy cell leukemia presenting as a peripancreatic mass: cytomorphology and radiographic correlates. *Acta Cytol* 2012; **56**:463–466.
89 Gibson G, Lai J, Thomas P. Unusual soft tissue infiltrates with 18F-FDG uptake in a patient with hairy cell leukemia. *Clin Nucl Med* 2015; **40**:e282–e284.
90 Robak P, Jesionek-Kupnicka D, Kupnicki P, Polliack A, Robak T. Multifocal osteolytic lesions in hairy cell leukemia–the importance of PET/CT in diagnosis and assessment. *Ann Hematol* 2021; **100**:1641–1645.
91 Doma A, Škerget M, Žagar I. 18F-FDG PET/CT for staging and evaluation of therapy in a patient with unusual hairy cell leukemia presentation. *Clin Nucl Med* 2019; **44**:e458–e460.
92 Bair SM, Brandstadter JD, Ayers EC, Stadtmauer EA. Hematopoietic stem cell transplantation for blood cancers in the era of precision medicine and immunotherapy. *Cancer* 2020; **126**:1837–1855.
93 Zeiser R, Blazar BR. Acute graft-versus-host disease–biologic process, prevention, and therapy. *N Engl J Med* 2017; **377**:2167–2179.
94 Pasquini M, Wang Z. *Current use and outcome of hematopoietic stem cell transplantation: CIBMTR summary slides*. Center for International, Blood & Marrow Transplant Research; 2015.
95 Deeg HJ. How I treat refractory acute GVHD. *Blood* 2007; **109**:4119–4126.
96 Bodet-Milin C, Lacombe M, Malard F, Lestang E, Cahu X, Chevallier P, *et al*. 18F-FDG PET/CT for the assessment of gastrointestinal GVHD: results of a pilot study. *Bone Marrow Transplant* 2014; **49**:131–137.
97 Dejanovic D, Amtoft A, Loft A. 18F-FDG PET/CT in extensive graft-versus-host disease of the gastrointestinal tract following autologous stem cell transplantation. *Diagnostics (Basel)* 2018; **8**:72.
98 Stelljes M, Hermann S, Albring J, Köhler G, Löffler M, Franzius C, *et al*. Clinical molecular imaging in intestinal graft-versus-host disease: mapping of disease activity, prediction, and monitoring of treatment efficiency by positron emission tomography. *Blood* 2008; **111**:2909–2918.
99 Roll W, Evers G, Strotmann R, Albring J, Reicherts C, Noto B, *et al*. Fluorodeoxyglucose F 18 for the assessment of acute intestinal graft-versus-host disease and prediction of response to immunosuppressive therapy. *Transplant Cell Ther* 2021; **27**:603–610.
100 Wang H, Cao F, Li J, Li Y, Liu X, Wang L, *et al*. Homing of cytokine-induced killer cells during the treatment of acute promyelocytic leukemia. *Int J Hematol* 2014; **100**:165–170.

101 Kil K-E, Ding Y-S, Lin K-S, Alexoff D, Kim SW, Shea C, *et al*. Synthesis and positron emission tomography studies of carbon-11-labeled imatinib (Gleevec). *Nucl Med Biol* 2007; **34**:153–163.
102 Wang T, Lin Q, Zhang Y, Xu Z, Shi D, Cheng Y, *et al*. Synthesis and biological evaluation of novel PET tracers [18F] AG120 & [18F] AG135 for imaging mutant isocitrate dehydrogenase 1 expression. *Bioorg Med Chem* 2022; **53**:116525.
103 Choi KH, Song JH, Kwak Y-K, Lee JH, Jang HS. Analysis of PET parameters predicting response to radiotherapy for myeloid sarcoma. *PLoS One* 2021; **16**:e0261550.
104 Zhao Z, Zhou Y, Wang J, Zhang T, Li J, Zhang B, *et al*. The value of ^{18}F-FDG PET/CT in the prediction of clinical outcomes of patients with acute leukemia treated with allogeneic hematopoietic stem cell transplantation. *Oncol Lett* 2020; **20**:1–1.
105 Paolini R, Bianchini E, D'Andrea E, Al-Nahhas A, Banti E, Muzzio PC, *et al*. FDG-PET detection of primary bone marrow large B-cell lymphoma in a patient with hairy cell leukemia. *Nucl Med Rev Cent East Eur* 2007; **10**:23–25.
106 Kudura K, Ritz N, Templeton AJ, Kissling M, Kutzker T, Foerster R, *et al*. Additional primary tumors detected incidentally on FDG PET/CT at staging in patients with first diagnosis of NSCLC: frequency, impact on patient management and survival. *Cancers (Basel)* 2023; **15**:1521.
107 Carter KR, Kotlyarov E. Common causes of false positive F18 FDG PET/CT scans in oncology. *Braz Arch Biol Technol* 2007; **50**:29–35.
108 Buck AK, Bommer M, Juweid ME, Glatting G, Stilgenbauer S, Mottaghy FM, *et al*. First demonstration of leukemia imaging with the proliferation marker 18F-fluorodeoxythymidine. *J Nucl Med* 2008; **49**:1756–1762.
109 Nikaki A, Papadopoulos V, Valotassiou V, Efthymiadou R, Angelidis G, Tsougos I, *et al*. Evaluation of the performance of 18F-fluorothymidine positron emission tomography/computed tomography (18F-FLT-PET/CT) in metastatic brain lesions. *Diagnostics (Basel)* 2019; **9**:17.
110 Holter JL, Thorp K, Smith ML, Kedzierska K, Fung K-MA, Chacko G, *et al*. [18F] fluorothymidine PET imaging in the diagnosis of leptomeningeal involvement with diffuse large B-cell lymphoma. *Cancer Imaging* 2011; **11**:140–143.
111 Sanghera B, Wong WL, Sonoda LI, Beynon G, Makris A, Woolf D, *et al*. FLT PET-CT in evaluation of treatment response. *Indian J Nucl Med* 2014; **29**:65–73.
112 Agool A, Schot BW, Jager PL, Vellenga E. 18F-FLT PET in hematologic disorders: a novel technique to analyze the bone marrow compartment. *J Nucl Med* 2006; **47**:1592–1598.
113 Osl T, Schmidt A, Schwaiger M, Schottelius M, Wester H-J. A new class of PentixaFor- and PentixaTher-based theranostic agents with enhanced CXCR4-targeting efficiency. *Theranostics* 2020; **10**:8264–8280.
114 Herhaus P, Habringer S, Philipp-Abbrederis K, Vag T, Gerngross C, Schottelius M, *et al*. Targeted positron emission tomography imaging of CXCR4 expression in patients with acute myeloid leukemia. *Haematologica* 2016; **101**:932–940.
115 Mayerhoefer ME, Jaeger U, Staber P, Raderer M, Wadsak W, Pfaff S, *et al*. [68Ga] Ga-Pentixafor PET/MRI for CXCR4 imaging of chronic lymphocytic leukemia: preliminary results. *Invest Radiol* 2018; **53**:403–408.
116 Buck AK, Haug A, Dreher N, Lambertini A, Higuchi T, Lapa C, *et al*. Imaging of C-X-C motif chemokine receptor 4 expression in 690 patients with solid or hematologic neoplasms using (68)Ga-Pentixafor PET. *J Nucl Med* 2022; **63**:1687–1692.
117 Habringer S, Lapa C, Herhaus P, Schottelius M, Istvanffy R, Steiger K, *et al*. Dual targeting of acute leukemia and supporting niche by CXCR4-directed theranostics. *Theranostics* 2018; **8**:369–383.
118 Inazu M. Choline transporter-like proteins CTLs/SLC44 family as a novel molecular target for cancer therapy. *Biopharm Drug Dispos* 2014; **35**:431–449.
119 von Eyben FE, Kairemo K. Meta-analysis of 11C-choline and 18F-choline PET/CT for management of patients with prostate cancer. *Nucl Med Commun* 2014; **35**:221–230.
120 Reske SN, Blumstein NM, Neumaier B, Gottfried H-W, Finsterbusch F, Kocot D, *et al*. Imaging prostate cancer with 11C-choline PET/CT. *J Nucl Med* 2006; **47**:1249–1254.
121 Qin C, Wu Z, Li J, Sun X, Lan X. Differences in uptake of 18F-FDG and 11C-choline in a case of acute myeloid leukemia. *Clin Nucl Med* 2016; **41**:799–801.
122 Cegla P, Scibisz-Dziedzic K, Witkowska K, Kubiak A, Wierzchoslawska E, Kycler W, *et al*. Detection of a second primary cancer in a 18F-fluorocholine PET/CT – multicentre retrospective analysis on a group of 1345 prostate cancer patients. *Nucl Med Rev Cent East Eur* 2022; **25**:25–30.
123 Kudura K, Kern B, Hoffmann MH, Antwi K. The use of 18F-choline-PET/CT in chronic lymphocytic leukaemia. *J Clin Imag Med Case Rep* 2022; **3**:1781–1782.
124 Al-Ibraheem A. Theranostics in developing countries: addressing challenges and potentials from training to practice. *World J Nucl Med* 2023; **22**:171–173.
125 Hofman MS, Lau WE, Hicks RJ. Somatostatin receptor imaging with 68Ga DOTATATE PET/CT: clinical utility, normal patterns, pearls, and pitfalls in interpretation. *Radiographics* 2015; **35**:500–516.
126 Alabed YZ. 68Ga-DOTATATE PET/CT incidentally detects relapsed chronic lymphocytic leukemia in patient with metastatic neuroendocrine tumor. *Clin Nucl Med* 2023; **48**:e78–e79.
127 Dong Y, Zhou H, Alhaskawi A, Wang Z, Lai J, Yao C, *et al*. The superiority of fibroblast activation protein inhibitor (FAPI) PET/CT versus FDG PET/CT in the diagnosis of various malignancies. *Cancers (Basel)* 2023; **15**:1193.
128 Huang R, Pu Y, Huang S, Yang C, Yang F, Pu Y, *et al*. FAPI-PET/CT in cancer imaging: a potential novel molecule of the century. *Front Oncol* 2022; **12**:854658.
129 Wu S, Lin Z, Shang Q, Pang Y, Chen H. Use of 68Ga-FAPI PET/CT for detecting myeloid sarcoma of the breast and assessing early response to chemotherapy. *Clin Nucl Med* 2022; **47**:549–550.
130 Cui Y, Wang Y, Wang S, Du B, Li X, Li Y. Highlighting fibroblasts activation in fibrosis: the state-of-the-art fibroblast activation protein inhibitor PET imaging in cardiovascular diseases. *J. Clin. Med* 2023; **12**:6033.
131 Herskovits EH. Artificial intelligence in molecular imaging. *Ann Transl Med* 2021; **9**:824.
132 Al-Ibraheem A, Mottaghy FM, Juweid ME. PET/CT in Hodgkin lymphoma: an update. *Semin Nucl Med* 2022; **53**:303–319.
133 Veziroglu EM, Farhadi F, Hasani N, Nikpanah M, Roschewski M, Summers RM, *et al*. Role of artificial intelligence in PET/CT imaging for management of lymphoma. *Semin Nucl Med* 2023; **53**:426–448.
134 Li H, Xu C, Xin B, Zheng C, Zhao Y, Hao K, *et al*. 18F-FDG PET/CT radiomic analysis with machine learning for identifying bone marrow involvement in the patients with suspected relapsed acute leukemia. *Theranostics* 2019; **9**:4730.
135 Dun Y, Huang G, Liu J, Wei W. ImmunoPET imaging of hematological malignancies: from preclinical promise to clinical reality. *Drug Discov Today* 2022; **27**:1196–1203.
136 Srideshikan SM, Brooks J, Zuro D, Kumar B, Sanchez J, Echavarria Parra L, *et al*. ImmunoPET, [^{64}Cu]Cu-DOTA-anti-CD33 PET-CT, imaging of an AML xenograft model. *Clin Cancer Res* 2019; **25**:7463–7474.
137 Neumaier B, Mottaghy FM, Buck AK, Glatting G, Blumstein NM, Mahren B, *et al*. 18F-immuno-PET: determination of anti-CD66 biodistribution in a patient with high-risk leukemia. *Cancer Biother Radiopharm* 2008; **23**:819–824.
138 Glekas AP, Pillarsetty NK, Punzalan B, Khan N, Smith-Jones P, Larson SM. In vivo imaging of Bcr-Abl overexpressing tumors with a radiolabeled imatinib analog as an imaging surrogate for imatinib. *J Nucl Med* 2011; **52**:1301–1307.
139 Madabushi SS, Brooks J, Zuro D, Kumar B, Sanchez J, Parra LE, *et al*. AML ImmunoPET: 64Cu-DOTA-anti-CD33 PET-CT imaging of AML in xenograft mouse model. *bioRxiv* 2019; **1**:635078.
140 Allen KJ, Jiao R, Li J, Beckford-Vera DR, Dadachova E. In vitro and in vivo characterization of ^{89}zirconium-labeled lintuzumab molecule. *Molecules* 2022; **27**:6589.
141 Wang X-y, Wang Y, Wu Q, Liu J-j, Liu Y, Pan D-h, *et al*. Feasibility study of 68Ga-labeled CAR T cells for in vivo tracking using micro-positron emission tomography imaging. *Acta Pharmacol Sin* 2021; **42**:824–831.
142 Sun P, Han Y, Hu K, Huang S, Wang M, Zhou K, *et al*. Synthesis and biological evaluation of Al [18F]-NOTA-IPB-PDL1P as a molecular probe for PET imaging of PD-L1 positive tumors. *Bioorg Chem* 2022; **122**:105682.
143 Jung K-H, Park JW, Lee JH, Moon SH, Cho YS, Lee K-H. 89Zr-labeled anti-PD-L1 antibody PET monitors gemcitabine therapy-induced modulation of tumor PD-L1 expression. *J Nucl Med* 2021; **62**:656–664.
144 Mishra A, Kumar D, Gupta K, Lofland G, Sharma AK, Banka DS, *et al*. Gallium-68-labeled peptide PET quantifies tumor exposure of PD-L1 therapeutics. *Clin Cancer Res* 2023; **29**:581–591.